

LEAN: graph-based pruning for convolutional neural networks by extracting longest chains

Richard Schoonhoven^{1,*} Allard A. Hendriksen¹ Daniël M. Pelt^{1,2} K. Joost Batenburg^{1,2}

¹Computational Imaging Group, Centrum Wiskunde & Informatica, Amsterdam, Netherlands

²Leiden Institute of Advanced Computer Science, Leiden, Netherlands

{richard.schoonhoven, allard.hendriksen, d.m.pelt, k.j.batenburg}@cw.nl

Abstract

Convolutional neural networks (CNNs) have proven to be highly successful at a range of image-to-image tasks. CNNs can be computationally expensive, which can limit their applicability in practice. Model pruning can improve computational efficiency by sparsifying trained networks. Common methods for pruning CNNs determine what convolutional filters to remove by ranking filters on an individual basis. However, filters are not independent, as CNNs consist of chains of convolutions, which can result in sub-optimal filter selection.

*We propose a novel pruning method, **LongEst-chAiN** (LEAN) pruning, which takes the interdependency between the convolution operations into account. We propose to prune CNNs by using graph-based algorithms to select relevant chains of convolutions. A CNN is interpreted as a graph, with the operator norm of each convolution as distance metric for the edges. LEAN pruning iteratively extracts the highest value path from the graph to keep. In our experiments, we test LEAN pruning for several image-to-image tasks, including the well-known CamVid dataset. LEAN pruning enables us to keep just 0.5%-2% of the convolutions without significant loss of accuracy. When pruning CNNs with LEAN, we achieve a higher accuracy than pruning filters individually, and different pruned substructures emerge.*

1. Introduction

In recent years, convolutional neural networks (CNNs) have become state-of-the-art machine learning models to solve a wide variety of tasks [27], including image classification [26], segmentation [41], and denoising [45].

On many occasions, high-accuracy CNNs require a large amount of memory and computational resources. Long evaluation times can limit the applicability of neural networks in real-time applications, and large memory requirements can limit the usefulness for memory- or energy-limited applications [46]. Small networks may be more applicable in such settings, but may lack accuracy.

Neural network *pruning* [36, 24] has recently gained popularity as a technique to reduce the size of neural networks [16, 3]. When pruning, the neural network is reduced in size by removing parameters while trying to maintain a high accuracy. A common pruning method for CNNs is to remove individual parameters [15]. However, removing individual parameters may not directly lead to improved computational efficiency in CNNs [37]. Because CNNs contain convolution operations, which are parameterized by a *filter* matrix, a convolution still needs to be performed when at least one filter parameter remains active. Therefore, to reduce computational effort, it is necessary to remove or keep entire filters, which is the focus of this work.

In this paper, we propose that instead of pruning parameters independently, we must take chains of interdependent operations into account. Specifically, we develop a pruning criterion for keeping or removing entire chains of operations. Convolutions can be mathematically represented as linear operators, which can be ranked by operator norm. The norm of a chain of convolutions can be estimated by multiplying the norms of the individual convolutions. We argue that when non-linearities are present, the product of the individual operator norms can still serve as a reasonable proxy for the effect of the entire chain. For image-to-image tasks, the operator norm can be computed readily. For classification tasks, the computation is technically more complex due to the changing dimensions of the feature maps across different layers of the network. We therefore focus on image-to-image tasks here.

Here, we present a novel pruning method called longest-chain (LEAN) pruning. In LEAN, a CNN is represented as a graph, with the operator norm of each convolution as

*Corresponding Author.

Financial support provided by The Netherlands Organization for Scientific Research (NWO), project numbers 639.073.506 and 016.Veni.192.235.

distance metric for the edges. We argue that the strongest subnetworks in a CNN can be discovered by extracting the longest paths, using linear time graph algorithms.

The advantages of LEAN pruning become apparent in a severe pruning regime, i.e., when a *pruning ratio* (percentage of remaining parameters after pruning) of 0.1–1% is used. In these severe pruning regimes, neural network pruning can result in *network disjointness*, i.e., suboptimal network structures that contain sections that are not part of some path from the input to the network output. Some existing pruning methods take into account network structure to a limited degree. For instance, some methods prune entire groups of filters [35, 31, 33]. These methods consider the decomposition of a CNN into layers and set separate pruning criteria for each. However, these methods do not contain safeguards to avoid network disjointness.

This paper is structured as follows. In section 2, we explore existing pruning approaches. In section 3, we outline the preliminaries on CNNs, pruning filters, and the operator norm. Next, in section 4, we introduce LEAN pruning. In section 6, we obtain experimental results for several datasets: (i) the CamVid dataset [5, 4]; (ii) a real-world dynamic CT dataset [6, 7]; and (iii) a simulated high-noise segmentation dataset. For the CT experiment, we report practically realized wall time speedup. Also, we discuss the various pruned substructures that arise from the pruning methods. Finally, we present our conclusions in section 7.

2. Related work

Reducing the size of neural networks by removing parameters has been studied for decades [36, 24, 17]. Neural network pruning can be used for compressing a network to reduce memory requirements [15, 13], and for creating computationally efficient networks [47, 33]. Recent results focus on sparsifying the individual parameters in a neural network [16], or prune filters at runtime based on the feature maps [29]. Alternatively, one can decide which channels to keep so that the feature maps approximate the output of the unpruned network over several training examples [33]. Apart from pruning the convolutional filters, it is possible to sparsify the parameters of other common components of CNNs, such as the batch normalization layers [47, 31, 21].

Many pruning approaches are aimed at reducing neural network size with very little accuracy drop [10, 19, 34, 48], as opposed to sacrificing accuracy in favour of computation speed. These approaches rarely exceed a theoretical computation speedup of a factor of 2–8 [3, 33, 30, 16]. When a high pruning ratio is used, e.g., a range 5–10% [29, 32], a significant drop in accuracy is observed. Pruning ratios of 2–10% can be achieved with an accuracy drop of 1–3% by learning-rate rewinding [40]. However, the reduction in FLOPs was less substantial (1.5–4.8 times), as individual parameters were pruned. A more extensive survey of the

many different pruning methods can be found in [3].

Criteria for deciding which elements of a neural network to prune have been extensively studied. A common choice is to use the L_1 -norm to score parameter importance. However, whether the magnitude of a parameter is a reasonable metric to rank neuron importance has been questioned [28]. In relation to the operator norm, several publications discuss computing the singular values of convolutional layers [44]. Singular values can be used to compress network layers [8], and for pruning feed-forward neural networks [1]. Furthermore, a definition of ReLU singular values was proposed recently with an accompanying upper bound [9].

Recently, the *lottery ticket hypothesis* was proposed, based on the idea that pruning exposes subnetworks (called *winning tickets*) that have been made effective through the random initialization [12]. However, it has been shown that retraining a pruned network with the “winning” initialization is not better than training the pruned network from scratch [32]. Instead, “the resulting pruned architectures are more likely to be what brings the benefit” [32]. At the end of this paper, we will briefly comment on the possibility of using LEAN for architecture discovery. Searching for efficient architectures using pruning has been done before [10].

3. Preliminaries

3.1. CNNs for segmentation

In this work, we demonstrate the results of the proposed pruning approach on a series of image segmentation problems. The goal of semantic image segmentation is to assign a class label to each pixel in an image. A segmentation CNN computes the function $f : \mathbb{R}^{m \times n} \rightarrow [0, 1]^{k \times m \times n}$, which specifies the probability of each pixel being in one of the k classes for an $m \times n$ image.

CNNs are predominantly composed of layers of convolution filters. Every layer takes output images of certain previous layers (starting from the input image), and convolves them with learned convolution filters. The CNN passes these convolved images to the next layers. The exact arrangement of layers, and connections between them, depends on the architecture. In addition, there are other types of layers such as pooling and batch normalization layers which are often used to increase accuracy. For an overview of CNN components we refer to [14].

A batch normalization layer [22] takes a feature map \mathbf{x}_i and scales and shifts it by

$$\mathbf{y}_i = \gamma \frac{\mathbf{x}_i - \mu_B}{\sqrt{\sigma_B^2 + \epsilon}} + \beta.$$

Here, γ and β are the batch normalization parameters and biases which are learned during training, and μ_B and σ_B^2 are the running mean and variance of the mini-batch, i.e.,

the set of images used for the current training step. When a convolutional channel is succeeded by a batch normalization channel, scaling the parameters of the convolution is undone. This observation has been called *transform invariance* [47]. Batch normalization influences the preceding convolution, and needs to be incorporated into the chain of dependent convolutions, as we discuss in section 4.2.

3.2. Pruning convolution filters

Pruning encompasses several techniques for removing parameters from a neural network. Several schemes exist to prune parameters from a neural network. When using one-shot pruning, the network is trained to convergence and then pruned once. Retraining the network after pruning is critical to avoid significantly impacting accuracy [16]. Instead of one-shot pruning, a neural network can be *fine-tuned*. Here, the network is repeatedly pruned by a certain percentage, until the desired pruning ratio is reached. Every step, the network is retrained for a few epochs. Fine-tuning typically gives better results than one-shot pruning [40].

Generic pruning algorithm: All pruning methods used in this work make use of the *fine-tuning* pruning algorithm outlined in Algorithm 1. The selection criteria for determining which filters to keep for each step defines the different pruning methods. The pruning ratio `pRatio` is the fraction of remaining convolutions we ultimately want to keep, and `stepRatio` is the fraction of convolutions that is pruned at each step.

Algorithm 1 Pruning algorithm

```

1: procedure PRUNE(MODEL, PRATIO, NSTEPS, EPOCHS)
2:   stepRatio  $\leftarrow e^{\ln(\text{pRatio})/nSteps}$ 
3:   for step  $\leftarrow 0$  to  $nSteps$  do
4:     pruneParams  $\leftarrow$  selectPrunePars(model, stepRatio)
5:     model  $\leftarrow$  removePars(model, prunedParams)
6:     for k  $\leftarrow 0$  to  $epochs$  do
7:       model  $\leftarrow$  trainOneStep(model, trainData)
   return model

```

A well-known approach for deciding which parameters are to be pruned is to use *magnitude pruning*, where the parameters with the lowest absolute value are pruned [16]. Alternatively, parameters can be pruned in a structured manner, e.g., prune entire filters or channels collectively. The threshold magnitude for the parameters to be pruned can be chosen per layer or globally. Global pruning gives higher accuracy than layerwise pruning for a certain pruning ratio [3].

In our experiments we refer to pruning a convolution filter $\mathbf{h} \in \mathbb{R}^{k \times k}$ by its L_1 vector norm $\|\mathbf{h}\|_1$, $\mathbf{h} \in \mathbb{R}^{k^2}$, as *individual filter pruning* (L_1). Note that the norm is in this case the sum of the absolute values of the parameters.

Note: When pruning individual filters in this work, we set the pruning thresholds globally.

3.3. Computing operator norms

As an alternative to the L_1 -norm, one can interpret a convolution as a linear operator which acts on the input feature maps, and score it according to an operator norm. A convolution operation on an image corresponds to a matrix multiplication. We denote by H the matrix associated to the convolution filter h .

As a metric for deciding which convolutions are to be pruned we use the (induced) operator norm $\|\cdot\|_p$

$$\|H\|_p := \sup \left\{ \|H\mathbf{x}\|_p \mid \mathbf{x} \in \mathbb{R}^n, \|\mathbf{x}\|_p = 1 \right\},$$

where $H\mathbf{x}$ denotes the application of convolution H (in matrix form) to image \mathbf{x} . In particular, we use the *spectral norm*, which is induced by the Euclidean norm ($p = 2$). The spectral norm can be obtained by calculating the largest singular value of the matrix $\|H\|_2 = \sigma_{\max}(H)$. Note that the spectral norm is submultiplicative, i.e., we have $\|AB\| \leq \|A\| \cdot \|B\|$ for all $A, B \in \mathbb{R}^{n \times n}$. Therefore, the norm of a chain of convolutions is approximated by multiplying the individual norms.

A substantially more efficient method than constructing H , is to obtain the singular value decomposition (SVD) of these convolutional matrices efficiently using the Fourier transform [44]. The matrix H is diagonalized by the two-dimensional unitary Discrete Fourier Transform (DFT), and the eigenvalues of H are given by the two-dimensional DFT of h^+ (see section 5 [23]). Here, h^+ is the filter matrix padded with zeroes to size $n \times n$. Practically, the singular values of H are the magnitudes of the complex entries of $F_{2D}(h^+)$. Here F_{2D} is the 2D Fourier transform.

$$\sigma_{\max}(H) = \max \left\{ |F_{2D}(h^+)| \right\}$$

Note that the Fourier-based method used in this work assumes a doubly-blocked circulant definition of H which corresponds to periodic boundary conditions as opposed to zero padding.

4. Method

4.1. LEAN: Creating the pruning graph

With a CNN, we associate a graph (the *pruning graph*), where the nodes correspond to the channels in the layers of the CNN, and the edges have weights corresponding to the scores used for pruning. If a channel takes input from a previous channel, we will construct a directed edge between those two nodes representing these channels. The score of the appropriate convolution is the value of the edge (see Figure 1). We use the spectral norm (see section 3.3) as a metric for the edges in this work, but other norms can be used as well.

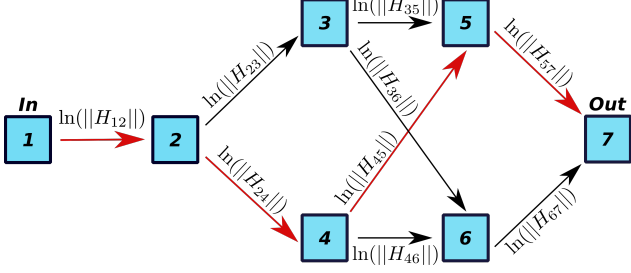


Figure 1: For a CNN, let h_{ij} be the convolution applied from channel i to j , with H_{ij} the associated matrix. Define the value of each edge as $\ln(\|H_{ij}\|)$. The logarithm is taken so that path lengths are multiplicative, instead of additive.

CNNs can contain skip connections which need to be incorporated in the graph. When skip connections are identity mappings, they are included by creating directed edges between the proper nodes with a value of 1. These skip connections do not represent prunable convolutions themselves, but are merely a tool to extract possible chains of convolutions. Sometimes skip connections are implemented as 1×1 convolutions. In this case, we include directed edges between the appropriate nodes, with the norms of these 1×1 convolutions as edge values. These types of skip connections are prunable.

4.2. LEAN: scaling the operator norm

If we interpret a convolution filter as an operator, we need to take the scaling of a succeeding batch normalization layer into account. As any operator norm satisfies $\|\lambda A\| = |\lambda| \|A\|$, we multiply the operator norm of each convolution, when it is succeeded by a batch normalization layer (see section 3.1), by

$$\left| \frac{\gamma}{\sqrt{\sigma_B^2 + \epsilon}} \right|.$$

Note that we do not include β in the computation of the operator norm, but rather interpret it as a separate bias term.

Individual filter pruning (SV): The scaled operator norm can also be used to prune filters individually, which we will do for comparison in our experiments. This type of pruning will be referred to as *individual filter pruning (SV)*.

4.3. LEAN: extracting chains from the graph

We propose a novel pruning method where we prune chains of convolutions based on paths in the graph; we keep the *highest operator norm paths* in the graph. More specifically, because convolutions are composed multiplicatively, we must retain the highest *multiplicative* operator norm paths. This is referred to as LongEst-chAiN (LEAN) pruning. When we perform LEAN pruning, we iteratively extract such paths from the graph until we have reached the pruning ratio. For all paths p in the network P , consisting

of convolutions $h \in p$, we iteratively extract

$$p^* = \arg \max_{p \in P} \left\{ \prod_{h \in p} \|h\| \right\} = \arg \max_{p \in P} \left\{ \sum_{h \in p} \ln(\|h\|) \right\}.$$

Algorithm 2 LEAN

```

1: procedure LEAN(MODEL, PRUNERATIO)
2:   graph  $\leftarrow$  createNormGraph(model)
3:   retainedConvs  $\leftarrow$  []
4:   while fractionRemainingConvs  $< 1 - \text{pruneRatio}$  do
5:     bestChain  $\leftarrow$  longestPath(graph)
6:     retainedConvs  $\leftarrow$  retainedConvs + bestChain
7:     graph  $\leftarrow$  removeFromGraph(graph, bestChain)
   return retainedConvs

```

The CNNs considered in this work do not contain recurrent connections, and can therefore be interpreted as directed acyclic graphs (DAGs). For DAGs, the longest (highest value) path in the graph can be found in $\mathcal{O}(|V| + |E|)$ time, where $|V|$ is the number of nodes, and $|E|$ is the number of edges [43]. It is possible to transform an additive longest path problem into a multiplicative longest path problem by recording the logarithm of each distance on each edge.

Remark: For experiments on networks with batch normalization, we prune a batch normalization channel after all the input convolutions to that channel are pruned.

4.4. Redundancy pruning

The running variance of a batch normalization channel tends to zero when the associated convolution channel only outputs homogeneous images. As a consequence, the scaling of the operator norm described in section 4.2 increases for the convolutional channel. This causes the norm to be artificially inflated, and the channel is not pruned. Therefore, when pruning *individual* filters with the operator norm, there can be negative interaction with batch normalization. This can happen when 1) the preceding input convolutions to a convolutional channel are all pruned; or 2) the convolution channel always outputs zero-images due to the ReLU activation function.

In the first case, the convolutional channel is essentially redundant but traditional pruning methods don't necessarily enforce connected convolutional paths to be kept or pruned together. In the second case, small values of the running variance of batch-normalization layers can be used to detect channels which are not "dead", but whose output is always zero after applying the ReLU activation function.

To rectify this behaviour, we introduced an auxiliary pruning step called *redundancy pruning*. We augment each pruning step with a pass where a convolution is pruned if: 1) all the preceding input convolutions are pruned; or 2)

the running variance of the associated batch normalization channel is below some threshold (10^{-10} by default). The redundancy pruning step is performed for all methods in this work, including pruning using the L_1 -norm. It is applied every time after the original pruning step.

5. Experimental setup

5.1. CNN architectures

In this section, we present two CNN architectures that are used in the experiments; the mixed-scale dense convolutional neural network (MS-D) network [39], and the fully-convolutional ResNet50 (FCN-ResNet50) [18]. The motivation for focusing on the MS-D and ResNet50 networks is that they represent two very different architectures. The MS-D network has few parameters and is narrow, the ResNet50 network has a much larger number of parameters and much wider layers. Both have a residual structure, which is interesting from a graph theory point of view. Furthermore, ResNet50 has batch normalization layers whereas the MS-D network does not.

5.1.1 Mixed-scale dense network

The MS-D network is a small, densely connected CNN of which we want to investigate emerging pruning structures. A layer at position i takes as input all the outputs of the previous layers, plus the input image. Each input image is convolved with a different learned convolution. Each of the convolutions in the MS-D network, except for the final layer, is a dilated convolution. A diagram of an MS-D network architecture is displayed in Figure 2. The MS-D network has a low number of parameters: a trained MS-D network of 100 layers has 45.756 parameters, which is substantially fewer than, e.g., 32.940.996 for ResNet50 [18].

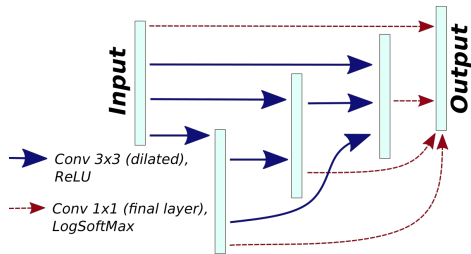


Figure 2: Diagram of 3-layer (typically has 100) MS-D network architecture.

5.1.2 Fully-convolutional ResNet

FCN-ResNet50 is a modern, widely used architecture. Fully-convolutional means that the ResNet has no final block of linear layers. A ResNet consists of subsequent convolutional layers arranged in blocks, and skip connections between certain blocks.

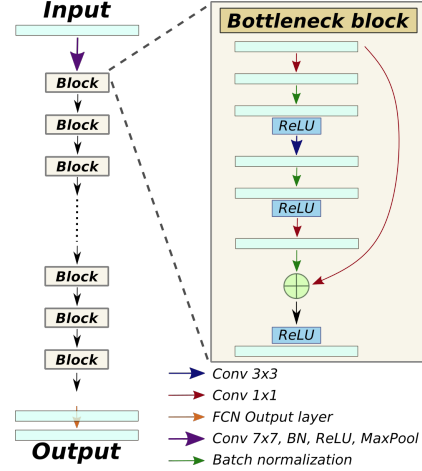


Figure 3: Diagram of FCN-ResNet50 architecture with bottleneck blocks. The network consists of 17 blocks. In every block, the input is passed through several layers of convolutions and batch normalization. In addition, a skip connection passes the feature map to the end of the block.

FCN-ResNet50 is comprised of bottleneck blocks (see Figure 3). For bottleneck blocks, the output of the previous block is added to the output of the last 1×1 convolution layer (after batch-normalization) before the activation function is applied. The skip connection inside the block is the identity function if no downsampling is applied in that layer. Otherwise, it is implemented as a 1×1 convolution with a stride larger than 1. In the FCN-ResNet segmentation architecture, every convolutional layer is succeeded by a batch-normalization layer [22], except for the final output layer. For more details see the original paper [18].

5.2. Datasets

For our experiments, we consider three datasets: a high-noise, but relatively simple, segmentation dataset; the complex, well-known CamVid dataset [5, 4]; and a real-world dynamic CT dataset to test the pruning methods in practice.

5.2.1 Simulated Circle-Square (CS) dataset

We used a simulated high-noise segmentation dataset containing 256×256 images of randomly placed squares and circles (CS dataset). The objects can be filled or hollow, creating a 5-class segmentation problem (see Figure 4). The objects were assigned a random grey value and Gaussian noise was added to the images. In total, we generated 1000 training, 250 validation, and 100 test images.

Experimental results on the CS dataset are quantified using global accuracy. We define global accuracy as the sum of all true positives and true negatives, divided by the total number of predictions. As a starting point for pruning, we trained an MS-D network with 100 layers which was able to obtain a global accuracy of 97.5%. FCN-ResNet50 was able to obtain an accuracy of 95.8% at convergence.

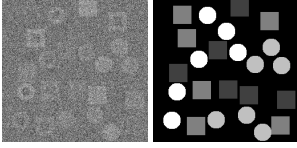


Figure 4: Example input and target images of the Circle-Square (CS) dataset.



Figure 5: Example input and target images of the CamVid dataset.

5.2.2 CamVid

The Cambridge-driving Labeled Video Database (CamVid) [5, 4] is a collection of videos with labels, captured from the perspective of a driving automobile. In total, 700 labeled frames are supplied at a resolution of 960×720 . The data is split into 367 training images, 100 validation images, and 233 test images. However, as the CamVid dataset contains few input images, we combined the training and validation datasets and trained for a fixed 500 epochs. Similar to other papers that apply CNNs to CamVid [4, 2, 38], we use 11 classes representing various roadside objects, and a single class representing unlabeled pixels (see Figure 5).

We used median frequency balancing [11] to balance classes for training, and set the class weight for *unlabeled* to zero. During training, we used data augmentation by randomly cropping and randomly (horizontally) flipping input images. Experimental results on the CamVid dataset are quantified using mean Intersection-over-Union (mIoU) [2, 38]. As a starting point for pruning, we trained an MS-D network with 150 layers which was able to obtain an mIoU of 0.5338. FCN-ResNet50 was able to obtain an mIoU of 0.6231.

5.2.3 Real-world dynamic CT dataset

Lastly, we used a real-world dynamic X-ray CT dataset of a dissolving tablet suspended in gel [6, 7]. The dataset contains noisy tomographic input images of rising air bubbles in a glass container filled with gel. The bubbles are to be segmented and separated from the noise and tomographic artifacts. The dataset is described in detail in [42]. The dataset consists of 512×512 images, split into 9216 training images, 2048 validation images, and 1536 test images. Example input and target images are shown in Figure 6.

The large amount of background pixels for this segmentation problem make global accuracy an unsuitable metric to properly distinguish methods. Therefore, we use the F1-

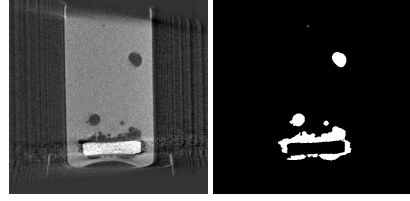


Figure 6: Example input and target images of the real-world dynamic CT dataset.

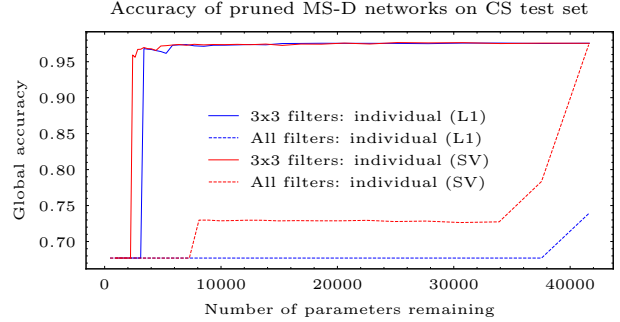


Figure 7: Global accuracy of pruned MS-D networks on the Circle-Square (CS) test dataset against the number of remaining parameters.

score (Dice coefficient). For our experiments we use the same MS-D architecture as used in [42]. The MS-D network that was used as a starting point for pruning achieved an F1-score of 0.8816.

5.3. Setup

We compare LEAN pruning to pruning individual filters using the L_1 -norm and spectral norm, denoted by *individual (L1)*, and *individual (SV)* respectively. We assess the performance of pruned neural networks across 5 independent runs of fine-tuning. The MS-D networks were pruned to a pruning ratio of 1% in 45 steps, and FCN-ResNet50 was pruned to a ratio of 0.1% in 30 steps. Both were retrained for 5 epochs after each step.

The MS-D network and FCN-ResNet50 are both implemented in PyTorch. We used an MS-D network [20] where the dilations in layer i were set to $1 + (i \bmod 10)$. Our model of the MS-D network has filter size 3×3 for all the convolutions, except the final 1×1 -layer. We set the number of channels for each layer to 1 [39]. For the dynamic CT experiment, we implemented an MS-D model in PyTorch which loads the unpruned parameters of a network, thereby allowing us to measure practically realized wall time.

The networks were trained using ADAM [25] with $lr = 0.001$, minimizing the negative log likelihood function. For each dataset, we have trained a single model as a starting point for pruning (see section 5.2). For every run of an experiment, the trained model was fine-tuned from the same base model. All experiments were run on a workstation with an AMD Ryzen 3800X processor and NVIDIA GeForce

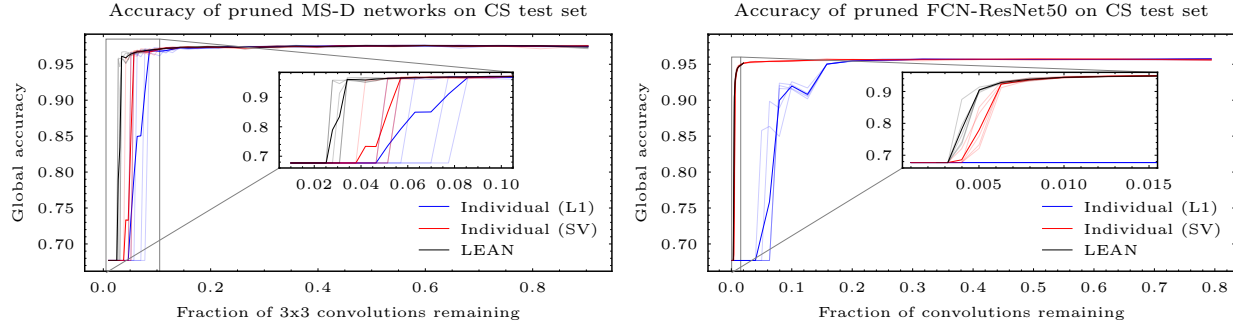


Figure 8: Global accuracy of pruned networks on the CS test dataset for individual filter pruning (both norms), and LEAN pruning. Displayed is the mean of 5 runs, with each individual run as a translucent line. Left: experimental results for MS-D networks (excluding the final output layer). Right: experimental results for ResNet50.

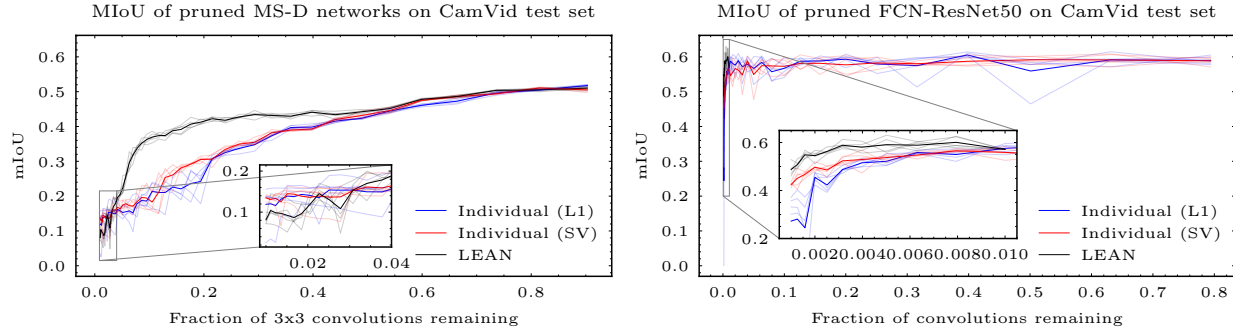


Figure 9: MIoU of pruned networks on the CamVid test dataset for individual filter pruning (both norms), and LEAN pruning. Displayed is the mean of 5 runs, with each individual run as a translucent line. Left: experimental results for MS-D networks (excluding the final output layer). Right: Experimental results for ResNet50.

RTX 2070 Super GPU, or on a server with two 8-core Xeon CPUs and four Titan X (12GB) GPUs.

Remark: Even though we use a linear time longest path algorithm, for each path extraction we need to re-run the longest path algorithm on the remaining graph. As a consequence, LEAN is computationally expensive on large CNNs. Therefore, ResNet50 was pruned with individual filter pruning using the spectral norm initially to reduce the size of the graph, before starting LEAN pruning. For the CS dataset, we started LEAN pruning from a ratio of 2%. For the more computationally expensive CamVid dataset, we started from a ratio of 1%.

6. Results

6.1. Effect of pruning individual convolutions

Before we present the main experimental results, we highlight the adverse effect pruning individual filters can have. In Figure 7 we show the accuracy of individual pruning for MS-D networks on the CS dataset. We compare between pruning the full networks, and excluding the final layer of 1×1 convolutions. For both norms (L_1 and SV), we observe that almost the entire final layer of 1×1 convo-

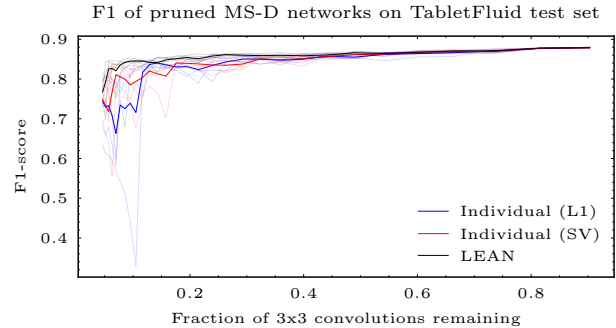


Figure 10: F1-score of pruned MS-D networks on the real-world dynamic CT test dataset against the fraction of pruned 3×3 -convolutions in the network.

lutions is immediately pruned, creating a disjoint network.

We observe that setting one global pruning threshold is detrimental to the pruning process, as the norms of the final layer have lower values than the other layers. This may be due to the different convolution dimensions, or zero-initialization of the final layer [39]. For the rest of the experiments on the MS-D network, we exclude the final layer from pruning to ensure a fair comparison.

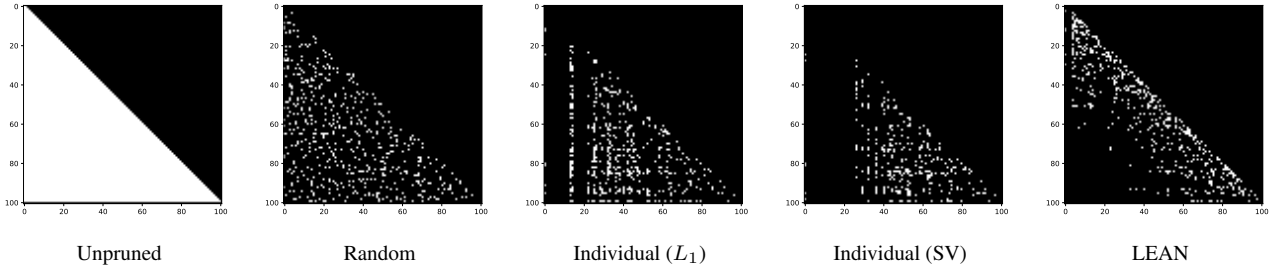


Figure 11: Adjacency matrices of active convolutions (in white) after pruning. All pruned network were pruned to a ratio of 10%. From left to right, we have the unpruned matrix of a 100-layer MS-D network trained on the real-world dynamic CT dataset, randomly pruned convolutions, individual (L_1), individual (SV), and LEAN.

6.2. Experimental results for severe pruning

In this section, we report on the pruning experiments on the CS and CamVid datasets. The results for the CS and CamVid datasets are displayed in Figure 8 and 9 respectively. LEAN pruning is able to create pruned networks with better accuracy and mIoU than individual L_1 and SV pruning. The pruning ratio that can be achieved without significant loss of accuracy for the MS-D network seems to depend on the problem complexity.

For the CS dataset, the MS-D network can achieve a pruning ratio of 3.4% with an average reduction in accuracy of 1.5% using LEAN pruning. On the other hand, on the CamVid dataset, the mIoU declines steadily as pruning progresses which may be due to the higher difficulty of the CamVid segmentation problem. On the CamVid dataset, there is a larger difference in performance between the networks pruned with LEAN and those pruned with individual L_1 or SV pruning.

For FCN-ResNet50, even though LEAN pruning started from pre-pruned networks, it was able to outperform the individual filter pruning methods. In particular, LEAN achieved a 0.5% pruning ratio with an accuracy reduction of on average 5.5% for CS, and an average mIoU reduction of 5.1% for CamVid. A notable highlight was that the best pruned network out of 5 achieved an mIoU of 0.6303 at a pruning ratio of 0.5%, which is *better* than the mIoU of the unpruned base network of 0.6231.

6.3. Speedup real-world dynamic CT segmentation

We performed a pruning experiment on the real-world dynamic X-ray CT dataset with the MS-D network. The comparison between individual filter pruning and LEAN pruning is shown in Figure 10. Again, we see that LEAN pruning outperforms both other methods. In particular, LEAN pruning achieved a pruning ratio of 5% with an F1-score drop of on average 10.2% for the TabletInFluid dataset. Notable highlight was an MS-D network which was able to achieve an F1-score of 0.8436 (drop of 4.3%) at a pruning ratio of 5%. This network was loaded into the

Batch size	Evaluation time (seconds)		Speedup
	Base MS-D	Pruned MS-D	
1	51.9 \pm 0.1	7.56 \pm 0.03	6.9x
6	66.0 \pm 0.0	5.86 \pm 0.03	11.3x

Table 1: Practically realized wall time speedup of pruned MS-D networks evaluated on the entire test dataset. The pruned network allows for a larger batch size.

Pruned-MSD model, and has a theoretical FLOPs reduction of 19.6. The practically realized wall time speedup is given in Table 6.3.

Finally, we show the adjacency matrices of MS-D networks pruned to a ratio of 10% in Figure 11. After pruning, LEAN retains only connections linked to nearby layers in the densely connected MS-D network. Compared to individual filter pruning, LEAN exposes a distinct structure which suggests that LEAN could be used for architecture discovery.

7. Conclusion

In this paper, we have introduced a novel pruning method (LEAN) for CNN pruning by extracting the highest value paths of convolutions. We incorporate existing graph algorithms, and computationally efficient methods for determining the operator norm. We show that LEAN pruning permits removing significantly more operations while retaining better network accuracy than pruning based on individual filters across different norms. Notably, in one instance, we were able to prune ResNet50 to a ratio of 0.5% for the CamVid dataset while obtaining a stronger network. Our results show that LEAN pruning can increase the speed of the network, both in theoretical speedup (FLOPs reduction) and in practice. Furthermore, visualizing the pruned MS-D architectures shows that LEAN exposes substantially different structures within CNNs than conventional pruning methods. In conclusion, LEAN enables severe pruning of CNNs while maintaining a high accuracy, by effectively exploiting the interdependency of network operations.

References

- [1] S. Abid, F. Fnaiech, and M. Najim. A new neural network pruning method based on the singular value decomposition and the weight initialisation. In *2002 11th European Signal Processing Conference*, pages 1–4, 2002. 2
- [2] Vijay Badrinarayanan, Alex Kendall, and Roberto Cipolla. Segnet: A deep convolutional encoder-decoder architecture for image segmentation. *IEEE transactions on pattern analysis and machine intelligence*, 39(12):2481–2495, 2017. 6
- [3] Davis Blalock, Jose Javier Gonzalez Ortiz, Jonathan Frankle, and John Gutter. What is the state of neural network pruning? *arXiv preprint arXiv:2003.03033*, 2020. 1, 2, 3
- [4] Gabriel J Brostow, Julien Fauqueur, and Roberto Cipolla. Semantic object classes in video: A high-definition ground truth database. *Pattern Recognition Letters*, 30(2):88–97, 2009. 2, 5, 6
- [5] Gabriel J Brostow, Jamie Shotton, Julien Fauqueur, and Roberto Cipolla. Segmentation and recognition using structure from motion point clouds. In *European conference on computer vision (ECCV)*, pages 44–57. Springer, 2008. 2, 5, 6
- [6] Sophia Bethany Coban and Felix Lucka. Dynamic 3D X-ray micro-CT data of a tablet dissolution in a water-based gel, 2019. 2, 6
- [7] Sophia Bethany Coban, Felix Lucka, Willem Jan Palenstijn, Denis Van Loo, and Kees Joost Batenburg. Explorative Imaging and Its Implementation at the FleX-ray Laboratory. *Journal of Imaging*, 6(4):18, 2020. 2, 6
- [8] Emily L Denton, Wojciech Zaremba, Joan Bruna, Yann LeCun, and Rob Fergus. Exploiting linear structure within convolutional networks for efficient evaluation. In *Advances in neural information processing systems*, pages 1269–1277, 2014. 2
- [9] S. Dittmer, E. J., and P. Maass. Singular values for relu layers. *IEEE Transactions on Neural Networks and Learning Systems*, pages 1–12, 2019. 2
- [10] Xuanyi Dong and Yi Yang. Network pruning via transformable architecture search. In *Advances in Neural Information Processing Systems*, pages 760–771, 2019. 2
- [11] David Eigen and Rob Fergus. Predicting depth, surface normals and semantic labels with a common multi-scale convolutional architecture. In *Proceedings of the IEEE international conference on computer vision*, pages 2650–2658, 2015. 6
- [12] Jonathan Frankle and Michael Carbin. The lottery ticket hypothesis: Finding sparse, trainable neural networks. *arXiv preprint arXiv:1803.03635*, 2018. 2
- [13] Yunchao Gong, Liu Liu, Ming Yang, and Lubomir Bourdev. Compressing deep convolutional networks using vector quantization. *arXiv preprint arXiv:1412.6115*, 2014. 2
- [14] Ian Goodfellow, Yoshua Bengio, Aaron Courville, and Yoshua Bengio. *Deep learning*, volume 1. MIT press Cambridge, 2016. 2
- [15] Song Han, Huizi Mao, and William J Dally. Deep compression: Compressing deep neural networks with pruning, trained quantization and huffman coding. *arXiv preprint arXiv:1510.00149*, 2015. 1, 2
- [16] Song Han, Jeff Pool, John Tran, and William Dally. Learning both weights and connections for efficient neural network. In *Advances in neural information processing systems*, pages 1135–1143, 2015. 1, 2, 3
- [17] Babak Hassibi, David G Stork, and Gregory J Wolff. Optimal brain surgeon and general network pruning. In *IEEE international conference on neural networks*, pages 293–299. IEEE, 1993. 2
- [18] K. He, X. Zhang, S. Ren, and J. Sun. Deep Residual Learning for Image Recognition. In *2016 IEEE Conference on Computer Vision and Pattern Recognition (CVPR)*, pages 770–778, 2016. 5
- [19] Yang He, Ping Liu, Ziwei Wang, Zhilan Hu, and Yi Yang. Filter pruning via geometric median for deep convolutional neural networks acceleration. In *Proceedings of the IEEE/CVF Conference on Computer Vision and Pattern Recognition (CVPR)*, 2019. 2
- [20] Allard A. Hendriksen. Mixed-scale dense networks for pytorch. https://github.com/ahendriksen/msd_pytorch, 2020. 6
- [21] Zehao Huang and Naiyan Wang. Data-driven sparse structure selection for deep neural networks. In *Proceedings of the European conference on computer vision (ECCV)*, pages 304–320, 2018. 2
- [22] Sergey Ioffe and Christian Szegedy. Batch normalization: Accelerating deep network training by reducing internal covariate shift. *arXiv preprint arXiv:1502.03167*, 2015. 2, 5
- [23] Anil K. Jain. *Fundamentals of Digital Image Processing*. Prentice-Hall, Inc., USA, 1989. 3
- [24] E. D. Karnin. A simple procedure for pruning back-propagation trained neural networks. *IEEE Transactions on Neural Networks*, 1(2):239–242, 1990. 1, 2
- [25] Diederik Kingma and Jimmy Ba. Adam: A method for stochastic optimization. *International Conference on Learning Representations (ICLR)*, 2014. 6
- [26] Alex Krizhevsky, Ilya Sutskever, and Geoffrey E Hinton. Imagenet classification with deep convolutional neural networks. In *Advances in neural information processing systems*, pages 1097–1105, 2012. 1
- [27] Yann LeCun, Yoshua Bengio, and Geoffrey Hinton. Deep learning. *nature*, 521(7553):436–444, 2015. 1
- [28] Yann LeCun, John S Denker, and Sara A Solla. Optimal brain damage. In *Advances in neural information processing systems*, pages 598–605, 1990. 2
- [29] Ji Lin, Yongming Rao, Jiwen Lu, and Jie Zhou. Runtime neural pruning. In *Advances in neural information processing systems*, pages 2181–2191, 2017. 2
- [30] Shaohui Lin, Rongrong Ji, Chenqian Yan, Baochang Zhang, Liujuan Cao, Qixiang Ye, Feiyue Huang, and David Doermann. Towards optimal structured CNN pruning via generative adversarial learning. In *Proceedings of the IEEE/CVF Conference on Computer Vision and Pattern Recognition (CVPR)*, 2019. 2
- [31] Zhuang Liu, Jianguo Li, Zhiqiang Shen, Gao Huang, Shoumeng Yan, and Changshui Zhang. Learning efficient convolutional networks through network slimming. In *Proceedings of the IEEE International Conference on Computer Vision*, pages 2736–2744, 2017. 2

- [32] Zhuang Liu, Mingjie Sun, Tinghui Zhou, Gao Huang, and Trevor Darrell. Rethinking the value of network pruning. *arXiv preprint arXiv:1810.05270*, 2018. 2
- [33] Jian-Hao Luo, Jianxin Wu, and Weiyao Lin. Thinet: A filter level pruning method for deep neural network compression. In *Proceedings of the IEEE international conference on computer vision*, pages 5058–5066, 2017. 2
- [34] Pavlo Molchanov, Arun Mallya, Stephen Tyree, Iuri Frosio, and Jan Kautz. Importance estimation for neural network pruning. In *Proceedings of the IEEE/CVF Conference on Computer Vision and Pattern Recognition (CVPR)*, 2019. 2
- [35] Pavlo Molchanov, Stephen Tyree, Tero Karras, Timo Aila, and Jan Kautz. Pruning convolutional neural networks for resource efficient inference. *arXiv preprint arXiv:1611.06440*, 2016. 2
- [36] Michael C Mozer and Paul Smolensky. Skeletonization: A technique for trimming the fat from a network via relevance assessment. In D. S. Touretzky, editor, *Advances in Neural Information Processing Systems 1*, pages 107–115. Morgan-Kaufmann, 1989. 1, 2
- [37] Jongsoo Park, Sheng Li, Wei Wen, Ping Tak Peter Tang, Hai Li, Yiran Chen, and Pradeep Dubey. Faster CNNs with direct sparse convolutions and guided pruning. *arXiv preprint arXiv:1608.01409*, 2016. 1
- [38] Adam Paszke, Abhishek Chaurasia, Sangpil Kim, and Eugenio Culurciello. Enet: A deep neural network architecture for real-time semantic segmentation. *arXiv preprint arXiv:1606.02147*, 2016. 6
- [39] Daniël M. Pelt and James A. Sethian. A mixed-scale dense convolutional neural network for image analysis. *Proceedings of the National Academy of Sciences*, 115(2):254–259, 2018. 5, 6, 7
- [40] Alex Renda, Jonathan Frankle, and Michael Carbin. Comparing rewinding and fine-tuning in neural network pruning. *arXiv preprint arXiv:2003.02389*, 2020. 2, 3
- [41] Olaf Ronneberger, Philipp Fischer, and Thomas Brox. U-Net: Convolutional networks for biomedical image segmentation. In *International Conference on Medical image computing and computer-assisted intervention*, pages 234–241, 2015. 1
- [42] R. Schoonhoven, J. W. Buurlage, D. M. Pelt, and K. J. Batenburg. Real-time segmentation for tomographic imaging. In *2020 IEEE 30th International Workshop on Machine Learning for Signal Processing (MLSP)*, pages 1–6, 2020. 6
- [43] Robert Sedgewick and Kevin Wayne. *Algorithms*. Addison-wesley professional, 4 edition, 2011. 4
- [44] Hanie Sedghi, Vineet Gupta, and Philip M Long. The singular values of convolutional layers. *arXiv preprint arXiv:1805.10408*, 2018. 2, 3
- [45] Chunwei Tian, Yong Xu, and Wangmeng Zuo. Image denoising using deep CNN with batch renormalization. *Neural Networks*, 121:461–473, 2020. 1
- [46] T. Yang, Y. Chen, and V. Sze. Designing energy-efficient convolutional neural networks using energy-aware pruning. In *2017 IEEE Conference on Computer Vision and Pattern Recognition (CVPR)*, pages 6071–6079, 2017. 1
- [47] Jianbo Ye, Xin Lu, Zhe Lin, and James Z Wang. Rethinking the smaller-norm-less-informative assumption in channel pruning of convolution layers. *arXiv preprint arXiv:1802.00124*, 2018. 2, 3
- [48] Chenglong Zhao, Bingbing Ni, Jian Zhang, Qiwei Zhao, Wenjun Zhang, and Qi Tian. Variational convolutional neural network pruning. In *Proceedings of the IEEE/CVF Conference on Computer Vision and Pattern Recognition (CVPR)*, 2019. 2